

See discussions, stats, and author profiles for this publication at: <https://www.researchgate.net/publication/26685548>

Electronic and Vibrational Circular Dichroism Spectra of Chiral 4-X-[2.2]paracyclophanes with X Containing Fluorine Atoms. J Phys Chem A 113:14851

ARTICLE in THE JOURNAL OF PHYSICAL CHEMISTRY A · AUGUST 2009

Impact Factor: 2.69 · DOI: 10.1021/jp9050066 · Source: PubMed

CITATIONS

7

READS

38

6 AUTHORS, INCLUDING:



France Lebon

Università degli Studi di Brescia

38 PUBLICATIONS 419 CITATIONS

SEE PROFILE



Giovanna Longhi

Università degli Studi di Brescia

100 PUBLICATIONS 965 CITATIONS

SEE PROFILE



Renzo Ruzziconi

Università degli Studi di Perugia

113 PUBLICATIONS 1,189 CITATIONS

SEE PROFILE

Electronic and Vibrational Circular Dichroism Spectra of Chiral 4-X-[2.2]paracyclophanes with X Containing Fluorine Atoms[†]

Sergio Abbate,^{*,‡} France Lebon,[‡] Roberto Gangemi,[‡] Giovanna Longhi,[‡] Sara Spizzichino,[§] and Renzo Ruzziconi^{*,§}

Dipartimento di Scienze Biomediche e Biotecnologie, Università di Brescia, Viale Europa 11, 25123 Brescia, Italy, and Dipartimento di Chimica, Università di Perugia, via Elce di Sotto 8, 06100 Perugia, Italy

Received: May 28, 2009; Revised Manuscript Received: July 1, 2009

The absorption IR and vibrational circular dichroism (VCD) spectra of both enantiomers of 4-X-[2.2]paracyclophanes (X = F, CH₂F, COCF₃) have been recorded in the mid-IR and CH stretching regions. The electronic CD (ECD) spectra have been collected as well. VCD spectra in the two IR regions, 900–1700 cm⁻¹ and 2700–3200 cm⁻¹, have been compared with the corresponding DFT calculated spectra. The absolute configuration assignment was confirmed as previously determined. We have shown that, to various extents, the VCD and ECD spectra bear some information on the relative mobility of the two phenyl rings and on the existence of different conformers for the X group. It has been observed that X = F and X = CH₂F groups do not change the conformational and electronic properties of the parent X = H and X = CH₃ molecules. The X = COCF₃ group brings in a large perturbation to the [2.2]paracyclophanes, and the role of fluorine is less important than that of oxygen.

Introduction

[2.2]Paracyclophanes are intriguing systems to study phenomena such as π - π -stacking of electronic orbitals and correlated phenomena,¹ like cask conformations induced by transannular interaction and aliphatic bridge strain. Also the twisting of one ring with respect to the other, in either direction, has been proposed for a long time and searched for. In particular the work of Grimme and collaborators^{2,3} has allowed clarification of these aspects and also description of the phenomena by high-level theory. The dependence of the phenomena on the substituents in various positions has also been investigated, and several spectroscopic works have been devoted to it throughout the years. Moreover, since the substitution at C-4 of [2.2]paracyclophane ([2.2]PC) makes the resulting molecule chiral, chiroptical techniques, like optical rotation (OR), electronic (ECD) and vibrational circular dichroism (VCD) spectroscopies, have been employed in the structural analysis of this class of compounds.^{4–8} The present work aims at investigating the geometrical, vibrational and electronic properties of 4-X-[2.2]paracyclophanes **1–3** (X = F (**1**), CH₂F (**2**), COCF₃ (**3**), Figure 1) by combining the experimental methods just mentioned above with DFT and TD-DFT calculations, performed by the Gaussian suite of programs.⁹ The three molecules are expected to provide information on increasing perturbations to the bare [2.2]PC scaffold. Indeed, fluorine is expected to perturb the structure of [2.2]PC so little that it allows to infer some properties of [2.2]PC; the CH₂F substituent is expected to behave like the previously studied CH₃ group;² finally the substituent COCF₃ should provide more evident perturbations. Moreover, we also expect to gain some insight in the behavior of fluorine, when it is inserted in a chiral organic context. This topic has

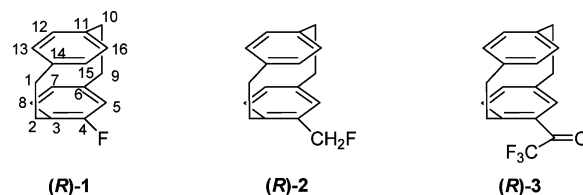


Figure 1. F- (**1**), CH₂F- (**2**) and CF₃C(=O) (**3**)-substituted [2.2]paracyclophanes. The atom numbering is provided for **1**.

received much attention in virtue of the importance of many fluoroorganic compounds in biology and pharmacology.¹⁰

Results and Discussion

As detailed in Experimental Details and Computations, (*R*)- and (*S*)-4-fluoro[2.2]paracyclophane were available from a previous work;⁶ both the enantiomers of 4-fluoromethyl[2.2]paracyclophane were obtained by DAST-promoted fluorination of the corresponding 4-hydroxymethyl derivatives. The latter were in turn prepared by reduction of the corresponding 4-carboxy[2.2]paracyclophane enantiomers⁶ with LiAlH₄. Both (*R*)- and (*S*)-4-trifluoroacetyl[2.2]paracyclophanes were obtained from the corresponding 4-bromo[2.2]paracyclophanes⁶ by butyllithium-promoted Br/Li exchange followed by the reaction of the resulting lithio-derivatives with ethyl trifluoroacetate.

As described later, we first calculated the geometries of the three 4-substituted [2.2]PC by GAUSSIAN03 at the B3LYP/TZVP level. In Table 1 we display the most relevant geometrical parameters, whose definition is given in Figure 2, that were built following the Grimme and Bahlmann model.² In Table 1 we report the dihedral angle τ , i.e. the driving angle used in Gaussian and defined in Table 1, and the dihedral angle defined by the four atoms: X–C⁴–C¹⁵–H¹⁵, (ϑ in Figure 2, X = F, COCF₃). We verified that the latter dihedral angle has the same value as the γ defined in ref 2 and depicted in Figure 2. Due to π - π transannular interactions, a cask shape can be assumed

[‡] Università di Brescia.

[§] Università di Perugia.

[†] Part of the "Vincenzo Aquilanti Festschrift".

* Corresponding authors. S.A.: tel, +39 030 3717415; fax, +39 030 3717416; e-mail: abbate@med.unibs.it.

TABLE 1: Calculated Values of the Geometrical Parameters c , d , d' , e , f , γ and τ Defined in Figure 2 for 4-X-[2.2]paracyclophanes^a

	F (1)	CH ₂ F(2a)	CH ₂ F(2b)	CH ₂ F(2c)	COCF ₃ (3a)
c (Å)	1.60	1.61	1.61	1.61	1.60
d (Å)	1.51	1.51	1.51	1.51	1.51
d' (Å)	1.51	1.52	1.52	1.51	1.51
e (Å)	3.10	3.19	3.17	3.22	3.18
f (Å)	2.82	2.83	2.83	2.83	2.82
γ (XCCH)	3.1°	2.5°	4.0°	3.1°	3.7°
τ (C ¹⁴ C ¹ C ² C ³)	13.4°	13.2°	13.9°	11.3°	18.9°
ΔG (kcal/mol)		0	0.3652	0.0289	
ΔE (kcal/mol)		0.5450	0.9239	0	
PoP ΔG		40%	22%	38%	
PoP ΔE		25%	13%	62%	99%

^a Geometric parameters are taken closest to the substituent group X, and we do not report the values for the other possible locations, since they were observed to be either coincident or quite close to the values reported here. For X = CH₂F we give also ΔG and ΔE values and relative population factors for the three conformers.

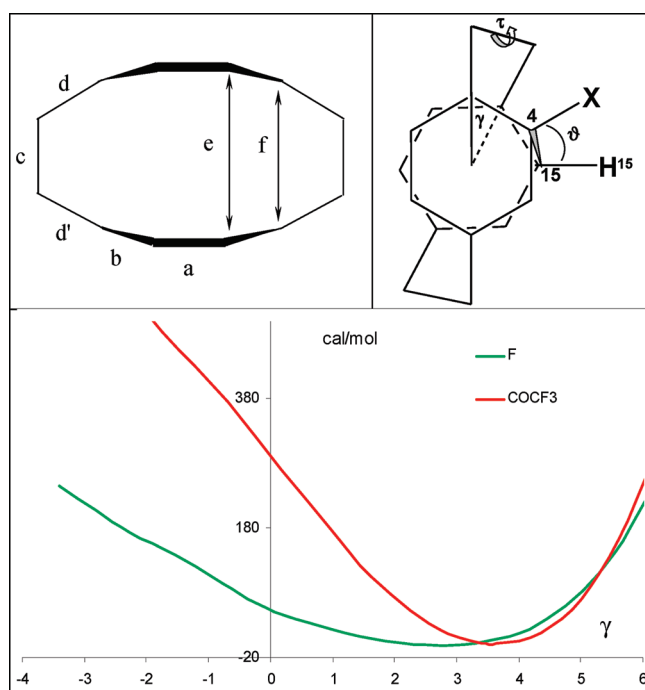


Figure 2. Definition of the geometrical parameters reported in Table 1 for [2.2]paracyclophane systems and calculated $E(\gamma)$ curves for 4-X-[2.2]paracyclophanes (X = F (1), COCF₃ (3)) around the vibrational minimum (see text and ref 2). The minimum dihedral angles γ (XCCH) for 1 and 3 are 3.1° and 3.7° respectively.

for such molecules;¹¹ this is indicated by the parameters e and f being different. Within the approximation used in Table 1 there is no difference between the three molecules; some effect may be noticed at a higher level of approximation where the [2.2]PC bearing the heavier CH₂F and COCF₃ substituents show a more pronounced deformation of the phenyl ring from planarity (we may call this effect “boating” effect). For 2 three conformations were computed (Figure 1b on page SI-15 in the Supporting Information); whereas in the case of 3 just one appreciably populated conformation was found (Figure 1c on page SI-15 in the Supporting Information), in accord with ¹H-, ¹³C-, and ¹⁹F NMR analysis. In the latter two cases the “boating” effect is more pronounced on the side of the X group. The twist angle γ of the unsubstituted ring with respect to the substituted one is quite similar in all three cases, while a significant distortion of the aliphatic τ (C¹⁴—C¹—C²—C³) dihedral angle is noticed in

the case of X = COCF₃. Our calculations, with functional and basis sets well tested to compute VCD spectra, give a value of $\gamma = 3.1^\circ$ for X = F, while Bahlmann and Grimme,² with a higher level method, the second-order Møller–Plesset perturbation theory, found a value of 9.4° (the experimental value for [2.2]-paracyclophane is 6°). More importantly, we did not observe the almost “enantiomeric” conformation for $\gamma = -3.1^\circ$, that was predicted by Bahlmann and Grimme to be at $\gamma = -9.4^\circ$ with a transition state next to $\gamma = 0^\circ$. However, we find that the energy profile $E(\gamma)$ reported in Figure 2 is quite flat, with energy values increasing by at most 0.3 kcal/mol within the range of $\Delta\gamma = \pm 5^\circ$ around the minimum at $\gamma = 3.1^\circ$. In addition, we observe that on the left of the minimum the curve slope is lower than on the right, which induces us to consider the possible existence of a second minimum (this could be assessed by other methods of calculus, but this is beyond the scope of the present work). In the plots in Figure 2 we superimpose the curves $E(\gamma)$ for the two extreme cases: [2.2]PC bearing the lightest substituent X = F and the heaviest one X = COCF₃. From these plots, we can deduce that the interconversion barrier between the two minima (in the case they existed) is very low and there is a large amplitude of the mutual torsional motion of the two phenyl rings. We think that the existence of such a torsional motion has consequences on the chiroptical data that will be examined later for the case X = F. For X = COCF₃ a more steeply increasing and more symmetric $E(\gamma)$ function can be observed with the minimum γ value slightly shifted (Figure 2). This means that the heaviest substituent is quite effective in stabilizing the relative angle of the two phenyl planes: the large torsional amplitude still does exist but is expected to be less important for X = COCF₃. Finally we wish to point out that to the $E(\gamma)$ curve, with γ defined in Figure 2, corresponds an $E(\tau)$ curve where τ is the CCCC dihedral angle for the aliphatic juncture of the two phenyl rings as defined in Table 1. In other words, while the two rings undergo a large amplitude torsion with respect to each other, the aliphatic junctures follow rather rigidly.

(a) VCD Spectra in Mid-IR Region. In Figure 3 we compare the experimental and calculated IR and VCD spectra in the mid-IR region for the three compounds under investigation. The comparison leaves no doubt about the assignment of the absolute configuration, which is (+) \leftrightarrow (R) for X = F, (−) \leftrightarrow (R) for X = CH₂F and (+) \leftrightarrow (R) for COCF₃.^{2,6,7} However, the correspondence between experimental and calculated spectra is not perfect for VCD and IR bands. This is probably due to conformational factors of the cyclophane structure and to the mobility of the X substituents. Let us make a more detailed analysis of the results for the three molecules.

(i) 1 (X = F). The IR spectrum resembles somehow the X-substituted [2.2]PC with X = Cl or I.⁸ Indeed, here and in all three cases of ref 8 there is a group of intense bands above 1350 cm^{-1} . Also below 1100 cm^{-1} an intense band appears that is common to all the molecules, whereas the intense band at 1250 cm^{-1} is typical of X = F: it is attributable to a quite delocalized normal mode involving C—F-stretching and also deformation modes of the aliphatic bridges. In the VCD spectra the bands common to all three cases (and also with other substituents, treated in ref 8) are the positive band at ca. 1100 cm^{-1} , the negative doublet at ca. 1300 cm^{-1} and the positive band at 1375 cm^{-1} . Instead, the three alternating couplets between 1120 and 1280 cm^{-1} are characteristic of X = F. The latter features were proved as being due to molecular vibrations containing large contributions from the C—F-stretching. The doublet at 1300 cm^{-1} originates in all cases X = F, Cl and I

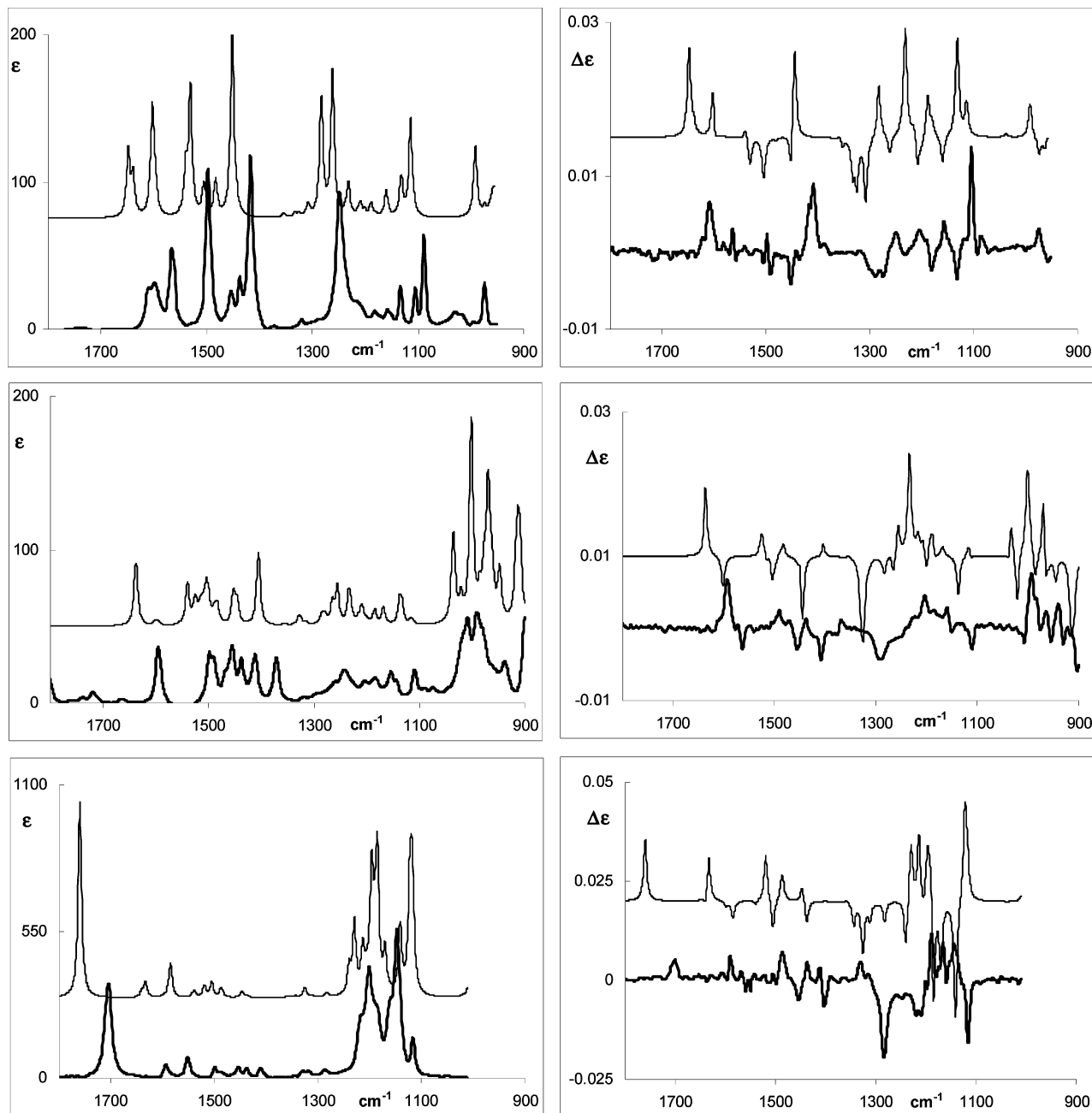


Figure 3. Comparison of experimental (bold trace) and calculated (lighter trace) IR (left) and VCD (right) spectra for 4-X-[2.2]paracyclophanes (X = F (**1**), top, X = CH₂F (**2**), middle, X = COCF₃ (**3**), bottom) in the mid-IR region. (See text.) Only the (*R*)-enantiomer reported. For X = CH₂F the average calculated spectra according to ΔG are reported.

from three normal modes, including in-plane HCC-bending motions of the aromatic rings coupled with CH₂-twisting modes of the methylenes, especially on the same side as the X group. These vibrations strongly depend on the relative positions of the two phenyl rings (Figure 2), and, since the function $E(\gamma)$ is quite flat, this allows for a large amplitude torsional motion. If, indeed, we run the calculations also for $\gamma = 5.5^\circ$ and $\gamma = -1.5^\circ$, that are both 0.14 kcal/mol above equilibrium, and superimpose them to the equilibrium value resulting for $\gamma = 3.1^\circ$, we find that the VCD spectra corresponding to the “shifted” geometries differ from those at the minimum not only for the discussed doublet but in the whole region 1150–1550 cm⁻¹, while the characteristic positive couplet at ca. 1100 cm⁻¹ is calculated to be the same for all geometries (instead the IR spectrum is not appreciably dependent on γ , apart from the calculated doublet above 1250 cm⁻¹ corresponding to a unique band observed at

1250 cm⁻¹). We also notice that the major changes are due to the geometry on the left of the minimum, where the $E(\gamma)$ function is increasing slowly. We observe from Figure 4 that the whole set of the calculated VCD spectra provides altogether a more satisfactory interpretation of the VCD data than the single calculated spectrum corresponding to γ at the minimum. A noticeable improvement of the predicted VCD spectrum is obtained by taking into account the calculated VCD for $\gamma = -1.5^\circ$, which is close to the second minimum predicted by Bahlman and Grimme.²

(ii) **2** (X = CH₂F). The IR spectrum in Figure 3, like those of the other [2.2]PC derivatives, still contains an intense group of ca. seven bands, and a quite intense and broad feature at ca. 1000 cm⁻¹, that is significantly more intense than those observed for the other [2.2]PCs. According to our normal-mode analysis, we attribute this group of bands to C–F stretching vibrations.

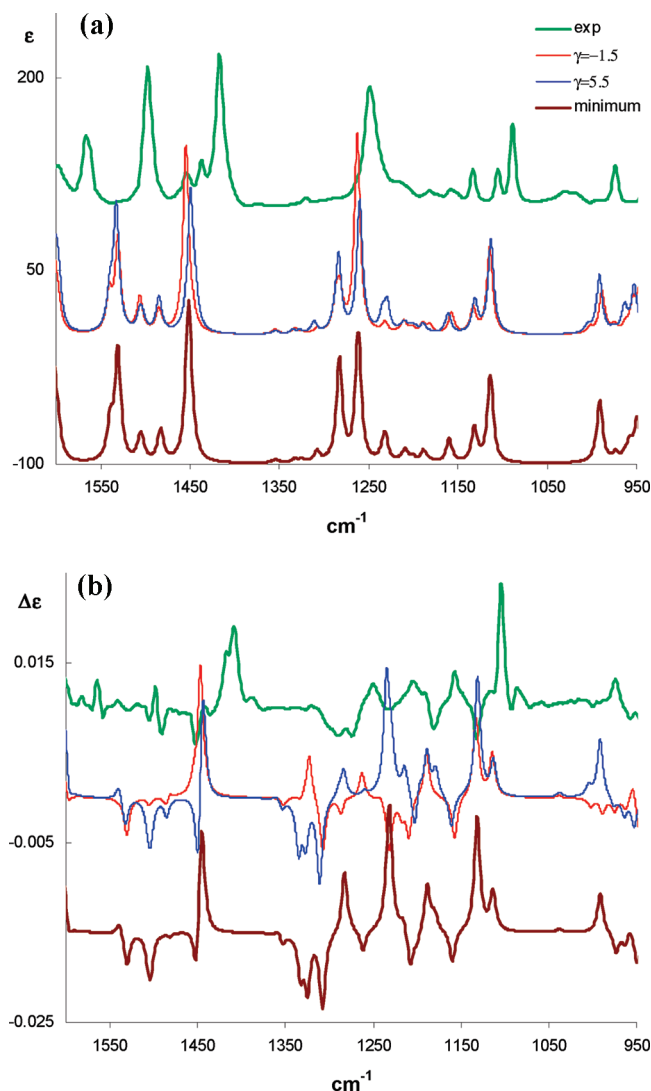


Figure 4. Comparison of experimental and calculated IR (top) and VCD (bottom) spectra for 4-fluoro[2.2]paracyclophane in the (*R*) absolute configuration for two pseudoconformers at $\gamma = +5.5^\circ$, $\gamma = -1.5^\circ$ and $\gamma = 3.1^\circ$ (minimum) (the former two values correspond to energies ca. 0.2 kcal/mol above the minimum).

Since fluorine is now bound to a saturated carbon rather than to the aromatic ring, the frequency is lower than that observed for $X = F$. The analysis of the VCD spectrum is even more intriguing. As in the previous case, the negative broad and structured feature at ca. 1300 cm^{-1} is due to phenyl HCC-bending combined with CH_2 -twisting motions. In this case too, because of the phenyl torsion, the VCD band shows a broadening, even though to a less extent than in the case of $X = F$. As it emerges from the data in Table 1, the conformer distribution is similar, even though the order in the population factors is different whether they are evaluated on the basis of ΔG or ΔE . This is one case where the experiment proves that the ΔG -based population factors are to be preferred. Indeed, the feature at ca. 1000 cm^{-1} is predicted only by assuming that the conformer **2a** is more populated than conformer **2c**, as predicted on the basis of ΔG values (Figure 2 on page SI-16 in the Supporting Information).

(iii) **3** ($X = \text{COCF}_3$). The most intense feature of the IR spectrum of this molecule is the $\text{C}=\text{O}$ stretching bands at 1706 cm^{-1} (calculated at 1750 cm^{-1}), followed by a group of three bands between 1250 and 1100 cm^{-1} . Their intensity is much higher than those observed in other [2.2]PC molecules. Aside from

the band calculated at ca. 1120 cm^{-1} , the calculations allow correct interpretation of the IR spectrum. The VCD spectrum is in even better agreement with calculations. Here, the phenomena pointed out above, being typical of the [2.2]PC derivatives, have the same interpretation.

(b) CH-Stretching Region. The comparison of calculated and experimental IR and VCD spectra is shown in Figure 5 (Figure 3 on page SI-16 in the Supporting Information reports the separate calculations for the conformers **2a–c**). In a previous work we provided calculation for the features below 2900 cm^{-1} in terms of Fermi resonance. Indeed, between 2900 and 2800 cm^{-1} , two major absorption bands and three evident VCD features with $(-, +, -)$ sign alternation can be observed. The same IR and VCD features were observed in ref 8 for other 4-*X*-[2.2]paracyclophanes: these IR and VCD features are thus independent of *X*. We conduct here just a harmonic analysis, and we assume that the same Fermi resonance anharmonic scheme presented in ref 8 is valid here, since no specific assumption on the substituent was made. The IR and VCD spectra above 2900 cm^{-1} are similar for $X = F$ and COCF_3 , and no significant effect in this region is observed by varying γ .

The spectra of compounds **1** and **3** resemble those of [2.2]PC derivatives with $X = \text{Cl}$, I , COOCD_3 , while they differ somewhat from those having $X = \text{CH}_2\text{F}$. In the latter case, we can observe that on one hand the additional CH_2 groups modify heavily the aliphatic CH normal mode scheme bringing in some additional features in the region typical of the C–H stretchings of the ethylenic bridges and, on the other hand, the major conformer according to ΔE (see Table 1) has a VCD spectrum which is different from that of the other two conformers (Figure 1b on page SI-15 and Figure 3 on page SI-16 in the Supporting Information).

(c) ECD Spectra. The interpretation of the ECD spectra follows closely that of the VCD spectra, since both data show the characteristic dependence on the geometrical parameters of the fundamental electronic state. Figure 6 shows the comparison between experimental and calculated (via TD-DFT) CD spectra of the three molecules in the $400\text{--}185\text{ nm}$ range. The calculations were performed with the same electronic ground state geometry used to calculate the VCD spectra in Figures 3 and 5, including 50 excited states.

For **1** ($X = F$) the results are quite similar to those of Grimme and Bahlmann.² In particular one notices that the assignment $(+) \leftrightarrow (R)$ is achieved by appropriately shifting the calculated features. In this way one obtains a good prediction, for the $^1\text{L}_b$ and $^1\text{L}_a$ doublets, as well as for the first component of the B_b doublet. Grimme and Bahlmann² attained slightly better results by including the calculated ECD spectra from the second conformer, whose existence they predicted. For this reason and similarly as done above for the VCD case, we calculated the ECD spectra corresponding to the two additional conformers with $\Delta E = 0.14\text{ kcal/mol}$ above the minimum at either side of the equilibrium position, thus allowing for some effect due to the large amplitude phenyl torsional motion. The results are not presented here, since they are quite similar to what obtained at equilibrium; the only significant change (as obtained also by Grimme and Bahlmann²) is the existence of a small positive feature that we calculate at ca. 290 nm for the pseudoconformers (one of them could be real) at $\gamma = -1.5^\circ$. This feature, which is not calculated for the γ value at the minimum (3.1° in our case) or for larger angles, is predicted also by Grimme and Bahlmann for $\gamma = -9.4^\circ$.

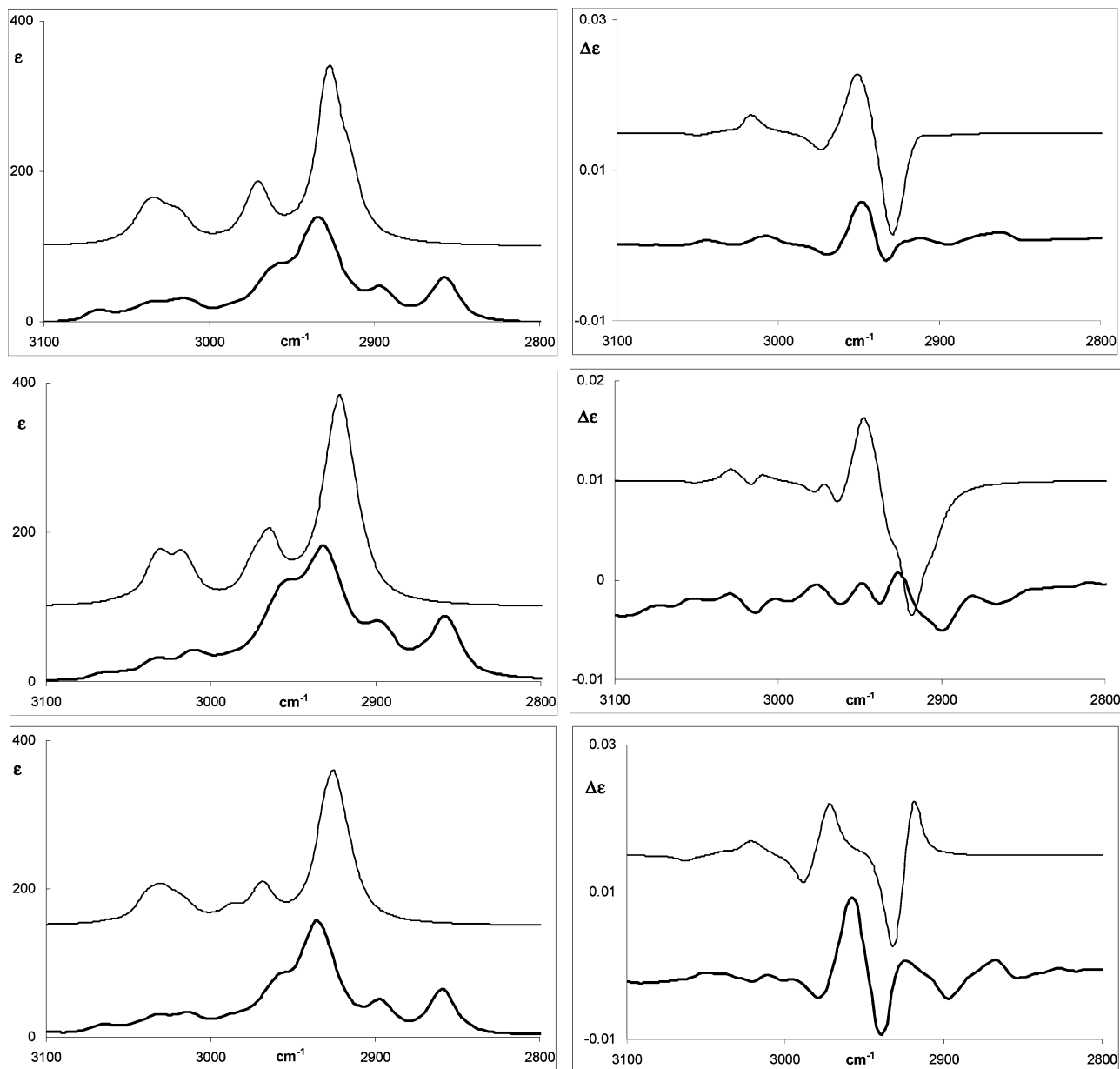


Figure 5. Comparison of experimental (bold trace) and calculated (lighter trace) IR (left) and VCD (right) spectra for 4-X-[2.2]paracyclophanes (X = F (**1**), top; X = CH₂F (**2**), middle; X = COCF₃ (**3**), bottom) in the CH-stretching region. (See text.) Only the (*R*)-enantiomer reported. For X = CH₂F the average calculated spectra according to ΔG are reported.

For **2** (X = CH₂F) (Figure 6) we calculated ECD spectra that are quite similar to the experimental ones, just as reported by Bahlmann and Grimme for the X = CH₃ case.² This proves that fluorine provides a small perturbation when replacing one hydrogen of the methyl group (it should be considered that the calculated spectrum is the average of three spectra derived from the corresponding conformers (Figure 4 on page SI-16 in the Supporting Information)). Still, a large torsional motion amplitude of the phenyl moiety could be envisaged, however, on the basis of the results obtained for **1**, we expect the calculated ECD spectra to be unaffected by this motion. This was found out also by Grimme and Bahlmann,² who showed that, for X = CH₃, calculated ECD spectra do not change appreciably by adding the contribution of the second conformer. The same considerations hold for the configurational assignment ((−) ↔ (*R*)) in this case) for X = F as well as for X = CH₃ as reported by Grimme and Bahlmann.

In the case of **3** (X = COCF₃), the observed ECD spectrum is dominated in intensity by the band at ca. 250 nm, character-

ized by a rotational strength value that is approximately twice as large as those observed in the other two cases. This feature is well matched, in wavelength and to a lesser extent in intensity, by the calculations (Figure 6 in this article and Figure 7 in the Supporting Information). Examining CI results we found that the $n \rightarrow \pi^*$ transition of the C=O moiety¹² contributes to the band of much smaller rotational strength at ca. 270 nm. The rest of the spectrum, originated from the [2.2]PC moiety, is subject to the same limitation as for **1** and **2**, namely, the calculated features should be shifted upward, in order to achieve good agreement between computed and experimental data. Anyway, the configurational assignment (+) ↔ (*R*) is even more reliable. In all three cases the quality of the results of the ECD spectra calculations is such that we cannot go beyond the comments of Grimme and Bahlmann² in interpreting their features simply in terms of coupled transition moments centered on the two phenyl moieties, as done e.g. by Rosini et al.⁷

Finally we observe that the signs of the optical rotation (OR) of both (*R*)-**1** (+34) and (*R*)-**2** (−72) are the same as those for

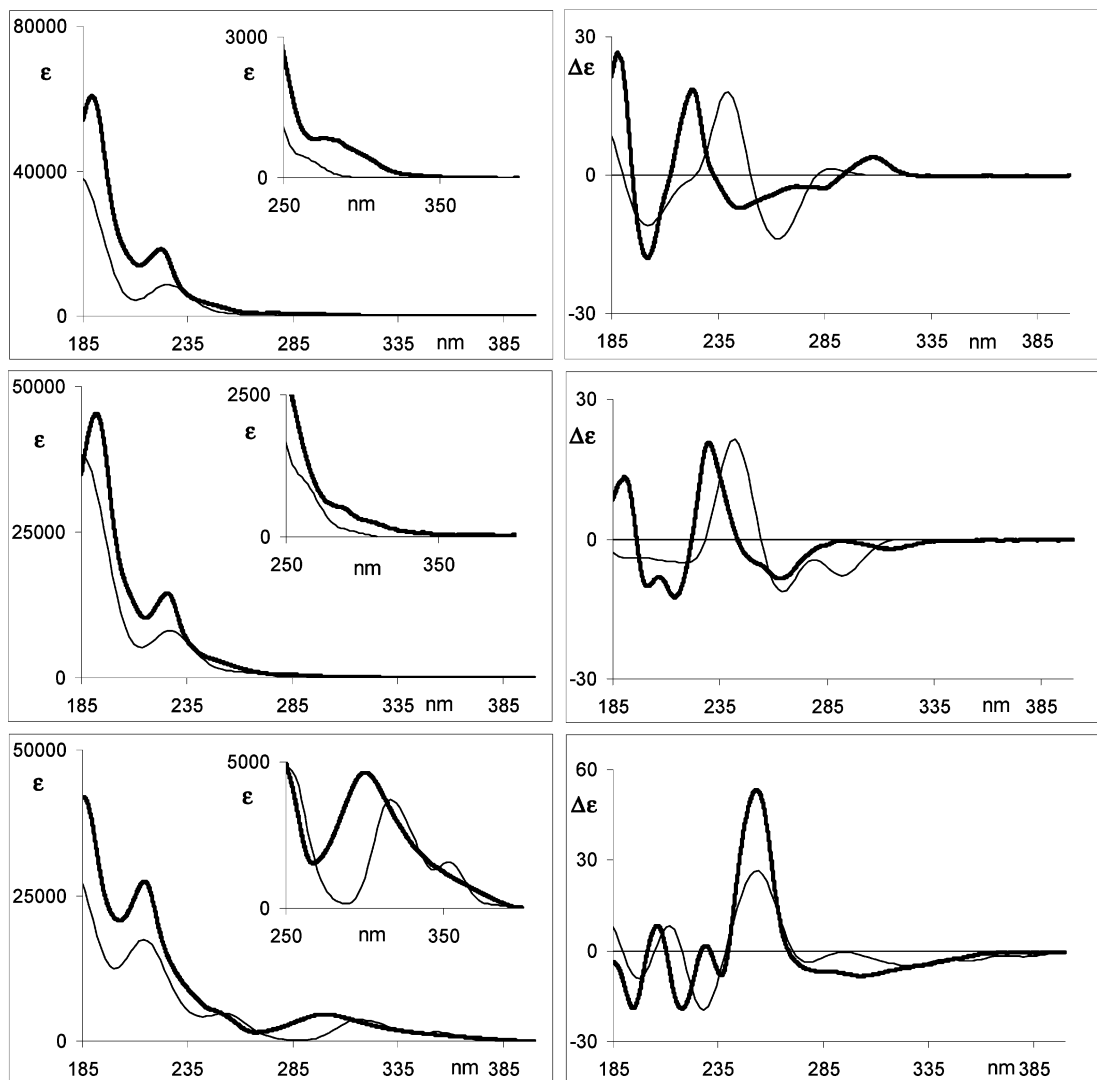


Figure 6. Comparison of experimental and calculated UV (left) and ECD (right) spectra for (*R*)-4-*X*-[2.2]paracyclophanes (*X* = F (**1**), top; *X* = CH₂F (**2**), middle; *X* = COCF₃ (**3**), bottom). For the experiment: dark trace. For the calculations: light trace. For *X* = CH₂F the average calculated spectra according to ΔG are reported.

the lowest wavelength observed ECD band, as pointed out by Rosini et al.,^{13a} who reasoned that the lowest lying transition is the one providing the largest denominator in the Rosenfeld's equation for the OR in terms of the CD intensities. The observed value of (*R*)-**3** (+2.8) is quite small. The observed signs can also be predicted on the basis of the simple model proposed by Ruzziconi et al.,⁶ whereby there is a simple relation between the polarizability P_X of the substituent *X* and the observed OR value, namely $P_X = -0.017[\alpha] + 1.58$, for a considerable number of *X* substituents. Indeed, by using the P_X values of Ma, Lii and Allinger¹⁴ and assuming the mean polarizability, a P_X value of 0.43 Å³ for *X* = F and 2.36 Å³ for *X* = CH₂F, respectively, can be calculated. By the correlation reported in ref 6 the calculated $[\alpha]$ values of +68 and -46 are obtained for *X* = F and *X* = CH₂F, respectively. A large discrepancy between experimental and calculated data is observed for *X* = COCF₃ based on the simple polarizability model. Here a P_X value of 4.38 Å³ can be obtained, which corresponds to $[\alpha] = -160$. This is strongly at odds with the small and positive experimental value ($[\alpha] = 2.8$). Preliminary TDDFT calculations do not give good results for the molecules here considered. Recently, it has been shown^{13c} that OR measurements and calculation at different wavelengths are required, especially if the OR measured value is small to see if the ORD curve is

monosigned. A systematic experimental and theoretical study taking into account also solvent effects is postponed to future investigations.

Conclusions

In this work we have determined the absolute configuration of three 4-*X*-[2.2]paracyclophanes with *X* containing fluorine atoms by a combination of experimental and theoretical methods, including VCD and ECD measurements and DFT and TD-DFT calculations.

The use of the chiroptical properties of a molecule in tandem with quantum mechanical calculations provides a powerful method for the determination of AC and the conformational properties. Among the others we just cite here refs 15–17 for VCD, and refs 18, 19 for ECD. These techniques allowed us also to get evidence of the presence of different conformers of *X*-substituent and, more importantly, to get evidence that the mutual torsional motion of the two phenyl rings has a substantial influence on some features of the spectra. For the F-substituted compound, whether this is related to the mobility or to the existence of a second conformer is beyond the sensitivity of our methods and requires further experimental evidence, even though the VCD spectrum, up to a certain point, indicates that

conformers possessing a relative dihedral angle between the two phenyls lower than at the minimum could also exist. A further evidence may come from NMR spectroscopy.²² In any case we expect at least some influence of the solvent on these conformational/mobility factors. We also wish to point out that the replacement of hydrogen by fluorine implies such a little, but strategic, perturbation to make 4-substituted-[2.2]paracyclophane as similar as possible to the [2.2]paracyclophane itself. The same can be said about the substitution of the CH₂F group replacing the CH₃ group in the 4 position of [2.2]PC. On the contrary, the COCF₃ group causes a more drastic perturbation, resulting in larger changes in ECD and VCD data.

Experimental Details and Computations

Synthesis and Characterization. ¹H, ¹³C and ¹⁹F NMR spectra were recorded at 400, 100, and 376 MHz, respectively, in CDCl₃ solution using tetramethylsilane as the internal standard. IR spectra were recorded with a FT-IR instrument on CHCl₃ solutions in the 4000–400 cm⁻¹ range. Gas-chromatographic analyses were performed using 30 m × 0.32 mm capillary columns loaded with two different stationary phases: HP-5 MS (5% phenyl-methylpolysiloxane) and HP-35 MS (5% phenyl-methylpolysiloxane) at 70–310 °C. Mass spectra were obtained at 70 eV. Optical rotation measurements were made on solutions at 20 °C, at the sodium D-line (589 nm). The optical purity of all products was checked by GLC analysis on a 30 m × 0.25 mm × 0.25 m BETADEx Supelco column.

Reagents. The parent **(R)-(-)-4-methoxycarbonyl[2.2]-paracyclophane** was prepared in practically quantitative yield by adding 1 M CH₂N₂ in ether (10 mL) to a solution of the corresponding acid²³ (1.00 g, 3.96 mmol) in diethyl ether (20 mL) until a persistent yellow color of the mixture was observed: mp 164–165 °C (from hexane); [α]_D²⁰ = -140 (c, 0.51); ¹H NMR δ 7.13 (d, *J* = 1.9 Hz, 1 H), 6.66 (dd, *J* = 7.9 and 1.8 Hz, 1 H), 6.5 (m, 5 H), 4.09 (ddd, *J* = 12, 9.7, and 1.8 Hz, 1 H), 3.91 (s, 3 H), 3.1 (m, 6 H), 2.86 (ddd, *J* = 13, 10, and 7.0 Hz, 1 H); ¹³C NMR δ 167.5, 142.6, 139.9, 139.8, 139.3, 136.4, 135.3, 133.1, 137.7, 132.2, 131.5, 130.6, 51.7, 36.1, 35.2, 35.1, 34.9; IR ν_{max} 3011, 2934, 2858, 1711, 1436, 1272, 1076, 712 cm⁻¹; MS, *m/z* (%) 266 (M⁺, 57), 251 (4), 162 (63), 147 (11), 119 (34), 104 (100), 78 (16). Elemental anal. Calcd for C₁₈H₁₈O₂: C, 81.17; H, 6.81. Found: C, 80.92; H, 6.74.

(S)-(+)-4-Methoxycarbonyl[2.2]paracyclophane: mp 163–165 °C; [α]_D²⁰ = +140 (c, 0.90), was prepared in the same way from optically pure (S)-(+)-4-carboxy[2.2]paracyclophane and exhibiting identical spectroscopic characteristics.

Both optically pure (R)-(-)- and (S)-(+)-4-bromo[2.2]-paracyclophane were available from a previous work.⁶ All the other commercial products of the highest purity grade were used without further purification. Tetrahydrofuran and diethyl ether were distilled from KOH pellets in the presence of CuCl and redistilled from sodium wire in the presence of the violet-blue benzophenone/sodium ketyl. CH₂Cl₂ was distilled from P₂O₅ after 2 h reflux.

(R)-(+)-4-Fluoro[2.2]paracyclophane was prepared in 45% yield from the corresponding (R)-(-)-4-amino[2.2]paracyclophane according to the procedure reported in the literature:⁶ mp 234–236 °C; [α]_D²⁰ = +34 (c, 1.2); ¹H NMR δ 6.9 (m, 1 H), 6.2 (m, 5 H), 5.90 (dd, *J* = 11 and 1.7 Hz, 1 H), 3.4 (m, 1 H), 3.2–2.9 (m, 6 H), 2.7 (m, 1 H); ¹³C NMR δ 161.1 (d, *J* = 245 Hz), 142.8 (d, *J* = 7.2 Hz), 139.7, 138.8, 135.4 (d, *J* = 6.3 Hz), 133.5, 132.9, 132.5, 129.1, 127.9 (d, *J* = 2.5 Hz), 125.8 (d, *J* = 18 Hz), 122.2 (d, *J* = 22 Hz), 35.2, 34.8, 34.2, 30.0; ¹⁹F NMR δ -112.9 (t, *J* = 8.9 Hz); IR ν_{max} 3016, 2997, 2983,

1206, 784 cm⁻¹; MS, *m/z* (%) 226 (M⁺, 13), 122 (18), 104 (100), 78 (14), 51 (5). Elemental anal. Calcd for C₁₆H₁₅F: C, 84.92; H, 6.68. Found: C, 85.01; H, 6.59.

(S)-(-)-4-Fluoro[2.2]paracyclophane was obtained in the same way (42%) starting from (S)-(+)-4-amino[2.2]paracyclophane: mp 233–235 °C; [α]_D²⁰ = -33 (c, 0.97). Elemental anal. Calcd for C₁₇H₁₅F: C, 84.92; H, 6.68. Found: C, 85.10; H, 6.69. The spectroscopic characteristics were identical to those of the (R) enantiomer.

(R)-(-)-4-Hydroxymethyl[2.2]paracyclophane. A solution of (R)-(-)-4-methoxycarbonyl[2.2]paracyclophane (0.70 g, 2.63 mmol) in dry THF (20 mL) was added dropwise, at 0 °C while stirring and under nitrogen atmosphere, to a suspension of LiAlH₄ (0.15 g, 3.95 mmol) in THF (5 mL). The mixture was allowed to react for 1 h before it was cautiously poured into ice water and acidified to pH ~ 3 with concentrated HCl. The organic product was extracted with diethyl ether (3 × 15 mL), and the collected organic phases were dried with Na₂SO₄. After the solvent evaporation at reduced pressure, chromatography of the residue on silica gel 60 (eluent, 1:1 light petroleum–diethyl ether) allowed the collection of the expected alcohol as white prism-shaped crystals (0.57 g, 91%) that were characterized as follows: mp 140–141 °C; [α]_D²⁰ = -67 (c, 0.84); ¹H NMR δ 6.59 (dd, *J* = 7.9 and 1.9 Hz, 1 H), 6.4 (m, 6 H), 4.70 (d, *J* = 13 Hz, 1 H), 4.38 (d, *J* = 13 Hz, 1 H), 3.39 (ddd, *J* = 13, 10, and 2.1 Hz, 1 H), 3.1 (m, 6 H), 2.86 (ddd, *J* = 13, 11, and 5.7 Hz, 1 H); ¹³C NMR δ 140.3, 139.7, 139.5, 139.2, 137.4, 135.0, 133.3, 133.2, 132.3, 132.1 (2×), 129.0, 64.5, 35.3, 35.0, 34.4, 32.8; IR ν_{max} 3607 (sharp, free OH group), 3300 (broad, associated OH group), 3010, 2932, 1231 cm⁻¹; MS, *m/z* (%) 238 (M⁺, 30), 220 (3), 134 (46), 119 (43), 105 (100), 104 (85), 91 (47). Elemental anal. Calcd for C₁₇H₁₈O: C, 85.67; H, 7.61. Found: C, 85.52; H, 7.49.

The same procedure, starting from (S)-(+)-4-methoxycarbonyl[2.2]paracyclophane (0.50 g, 1.9 mmol), allowed us to obtain **(S)-(+)-4-hydroxymethyl[2.2]paracyclophane** (0.46 g, 92%): mp 139–141 °C; [α]_D²⁰ = +67 (c, 0.78). Elemental anal. Calcd for C₁₇H₁₈O: C, 85.67; H, 7.61. Found: C, 85.30; H, 7.55. The spectroscopic characteristics were identical to those of the (R) enantiomer.

(R)-(-)-4-(Fluoromethyl)[2.2]paracyclophane. (Diethylamino)sulfur trifluoride (DAST) (0.26 mL, 2.0 mmol) was added at 0 °C under nitrogen atmosphere, by a syringe, to a solution of (R)-(-)-4-hydroxymethyl[2.2]paracyclophane (0.50 g, 2.1 mmol) in CH₂Cl₂ (10 mL). After 1 h, the mixture was poured into water (10 mL) and extracted with CH₂Cl₂ (3 × 15 mL), and the collected organic phases were dried with Na₂SO₄. After the solvent evaporation at reduced pressure, chromatography of the crude on silica gel 60 (eluent 8:2 light petroleum–diethyl ether) allowed the collection of the expected product (0.20 g, 40%) as white needles exhibiting the following spectroscopic and analytical characteristics: mp 129 °C (dec); [α]_D²⁰ = -72 (c = 0.50); ¹H NMR δ 6.4 (m, 7 H), 5.44–5.07 (eight peaks, AB portion of an ABX system, *J*_{AB} = 11 Hz, *J*_{AX} = 48 Hz, 2 H), 3.35 (t, *J* = 11 Hz, 1 H), 3.0 (m, 7 H); ¹³C NMR δ 140.3, 139.6, 139.2, 138.3, 135.0, 134.6, 133.5, 133.4, 133.1, 133.0, 132.2, 130.1, 84.0 (d, *J* = 163 Hz), 35.1, 34.8, 34.4, 32.5; ¹⁹F NMR δ -134.94 (t, X portion of an ABX system, *J*_{AX} = 48 Hz); IR (CDCl₃) ν_{max} 3045, 3031, 2932, 2858, 1596, 1256, 979 cm⁻¹; MS *m/z* (%) 240 (M⁺, 37), 136 (41), 115 (10), 104 (100), 78 (13). Elemental anal. Calcd for C₁₇H₁₇F: C, 84.96; H, 7.13. Found: C, 85.27; H, 7.03. Starting from (S)-(+)-4-hydroxymethyl[2.2]paracyclophane (0.50 g, 2.1 mmol), **(S)-(+)-4-(fluoromethyl)[2.2]paracyclophane** (0.21 g, 42%) was ob-

tained: mp 128 °C (dec); $[\alpha]_{\text{D}}^{20} = +71$ (c, 0.57). Elemental anal. Calcd for $\text{C}_{17}\text{H}_{17}\text{F}$: C, 84.96; H, 7.13. Found: C, 85.31; H, 6.99. The spectroscopic characteristics were identical to those of the corresponding (*R*) enantiomer.

(*R*)-(+)-4-(Trifluoroacetyl)[2.2]paracyclophane. Butyllithium (1.62 M in hexanes, 0.65 mL, 1.05 mmol) and, successively, ethyl trifluoroacetate (0.15 g, 1.05 mmol) were added at -75 °C, under argon atmosphere, to a solution of (*R*)-(-)-4-bromo[2.2]paracyclophane (0.30 g, 1.05 mmol) in THF (5 mL). The cold bath was removed and, after the temperature had reached 25 °C, the mixture was poured into water (20 mL) and extracted with diethyl ether and the collected organic phases were dried with Na_2SO_4 . The solvent was evaporated at reduced pressure, and the residue was chromatographed on silica gel 60 (eluent, 9:1 light petroleum–diethyl ether) to collect the expected trifluoroacetyl derivative as white needles (0.18 g, 56%): mp 80–81 °C; $[\alpha]_{\text{D}}^{20} = +2.8$ (c 0.58); ^1H NMR δ 7.11 (broad s, 1 H), 6.79 (dd, $J = 7.9$ and 1.6 Hz, 1 H), 6.63 (d, $J = 7.9$, 1 H), 6.59–6.51 (split AB system, $^3J_{\text{AB}} = 7.9$ and $^4J = 1.7$ Hz, 2 H), 6.45–6.36 (split AB system, $^3J_{\text{AB}} = 7.9$, $^4J = 1.7$ Hz, 2 H), 3.9 (m, 1 H), 3.2 (m, 4 H), 3.0 (m, 2 H), 2.9 (m, 1 H); ^{13}C NMR δ 181.2, 145.4, 140.2, 139.9, 139.3, 138.8, 136.9, 134.6, 132.9 (2 \times), 132.4, 131.3, 130.0, 116.5 (q, $J = 291$ Hz), 36.2, 35.0 (2 \times), 34.5; ^{19}F NMR δ -71.12 (d, $J = 1.9$ Hz); IR (CHCl_3) ν_{max} 1708, 1204, 1137 (CF_3) cm^{-1} ; MS, m/z (%) 304 (M^+ , 16), 200 (4), 131 (15), 104 (100), 77 (28). Elemental anal. Calcd for $\text{C}_{18}\text{H}_{15}\text{F}_3\text{O}$: C, 71.05; H, 4.97. Found: C, 71.23; H, 5.07.

Starting from (*S*)-(+)-4-bromo[2.2]paracyclophane (0.30 g, 1.05 mmol), the same procedure allowed us to obtain (*S*)-(-)-4-(trifluoroacetyl)[2.2]paracyclophane (0.16 g, 49%): mp 79–81 °C; $[\alpha]_{\text{D}}^{20} = -2.7$ (c, 0.63). Elemental anal. Calcd for $\text{C}_{18}\text{H}_{15}\text{F}_3\text{O}$: C, 71.04; H, 4.97. Found: C, 71.13; H, 7.12. The spectroscopic characteristics were identical to those reported above for the (*R*) enantiomer.

VCD Spectra. The VCD spectra were recorded on a JASCO 4000 FVS apparatus on both enantiomeric forms (*R*) and (*S*) of each compound dissolved in a variety of chlorinated solvents, namely, CCl_4 , CDCl_3 or CD_2Cl_2 solutions. For simplicity we report just the difference $(1/2)(R - S)$, after checking that they exhibit mirror image aspect. No appreciable differences were noticed between the measurements in different solvents (CCl_4 , CD_2Cl_2) for $\text{X} = \text{CH}_2\text{F}$. For $\text{X} = \text{COCF}_3$ we report the data for CD_2Cl_2 solutions which had to be used to avoid degradation of the sample. This fact limits to 1010 cm^{-1} the mid-IR region investigated for the last compound. The CH-stretching region (3200–2700 cm^{-1}) and the mid-IR region were investigated separately, using two different detectors (InSb and MCT respectively), on ~ 0.2 – 0.5 M or ~ 0.1 M concentrated solutions and with 0.1 mm or 0.5 mm path length cells, respectively. In the former case 10,000 scans, in the latter 4000 scans were taken for each measurement. For $\text{X} = \text{COCF}_3$ the carbonyl stretching region was treated separately (using a filter to collect signals only in the region 1550–1900 cm^{-1}) and added to the mid-IR spectra reported in the figures.

ECD Spectra. The ECD spectra were recorded on a JASCO 815SE apparatus with 5 scans each on ~ 0.003 M solutions in 0.1 mm path length cells. Samples were solved in CH_2Cl_2 (205–400 nm) and CH_3CN (185–400 nm), and no difference has been noted. The spectra were solvent subtracted.

DFT Calculations. The Gaussian03 suite of programs was used throughout. Due to the goals of the present work, we present the results for B3LYP/TZVP, which allow a balance between relative precision and economy. Gaussview has allowed

us to easily define the parameters of Table 1. Finally we calculate the electronic energy values at discrete points in the dihedral angle $\tau(\text{C}^{14}-\text{C}^1-\text{C}^2-\text{C}^3)$ along the aliphatic bridge close to the substituent, optimizing with respect to all other internal coordinates. From each calculated geometry we obtained the angle γ of Figure 2 (which has practically the same value as the HCCX angle) and therefrom we derived the continuous energy profile $E(\gamma)$ reported in Figure 2 that is central to our investigations. By DFT we calculated dipole and rotational strengths following the method implemented by Stephens²⁴ and obtained IR and VCD spectra assigning Lorentzian band-shapes to calculated dipole and rotational strengths at the calculated wavenumbers with $\Delta\nu = 8$ cm^{-1} in the mid-IR region and $\Delta\nu = 16$ cm^{-1} in the CH-stretching region ($\Delta\nu$ being the bandwidth). The same cases dealt with to obtain VCD spectra were also treated by TDDFT to obtain ECD calculated spectra: fifty singly excited states have been considered, rotational strength has been calculated in both the velocity and length formalisms obtaining almost identical results. From calculated dipole and rotational strengths, extinction coefficients ϵ and $\Delta\epsilon$ can be evaluated. We have assumed for each electronic transition a Gaussian band of 9 nm width.

Acknowledgment. We acknowledge financial support from Italian Ministry of Educational and University Research (MIUR) through PRIN Programs and Ms. Mara Salvi for helping to compose the text of the manuscript.

Supporting Information Available: NMR spectra of compounds **1**, **2**, **3**. Calculated geometrical structures of the three compounds. Calculated VA and VCD spectra for the possible conformers for compounds **2** and **3**. Calculated ECD spectra for the possible conformers for compounds **2** and **3**. This material is available free of charge via the Internet at <http://pubs.acs.org>.

References and Notes

- (1) (a) Vögtle, F. In *Cyclophane Chemistry, Synthesis, Structure and Reactions*; J. Wiley & Sons Ltd.: Chichester, 1993; Chapter 2, pp 71–112. (b) Hopf, H.; Marquard, C. In *Strain and its Implications in Organic Chemistry*; de Meijere, A., Bleichert, S., Eds; Kluwer: Dordrecht, 1989; p 297.
- (2) Grimme, S.; Bahlmann, A. Electronic Circular Dichroism of Cyclophanes, In *Modern Cyclophane Chemistry*; Gleiten, R., Hopf, H., Eds.; Wiley-VCH: 2004; Chapter 12, pp 311–336.
- (3) Furche, F.; Ahlrichs, R.; Wachsmann, C.; Weber, E.; Sobank, A.; Vogtle, F.; Grimme, S. *J. Am. Chem. Soc.* **2000**, *122*, 1717–1724.
- (4) Furo, T.; Mori, T.; Wada, T.; Inoue, Y. *J. Am. Chem. Soc.* **2005**, *127*, 8242–8243.
- (5) Furo, T.; Mori, T.; Origane, Y.; Wada, Izumi, H.; T.; Inoue, Y. *Chirality* **2006**, *18*, 205–211.
- (6) Cipiciani, A.; Fringuelli, F.; Mancini, V.; Piermatti, O.; Pizzo, F.; Ruzziconi, R. *J. Org. Chem.* **1997**, *62*, 3744–3747.
- (7) Rosini, C.; Ruzziconi, R.; Superchi, S.; Fringuelli, F.; Piermatti, F. *Tetrahedron: Asymmetry* **1998**, *9*, 55–62.
- (8) Abbate, S.; Castiglioni, E.; Gangemi, F.; Gangemi, R.; Longhi, G.; Ruzziconi, R.; Spizzichino, S. *J. Phys. Chem. A* **2007**, *111*, 7031–7040.
- (9) Frisch, M. J.; Trucks, G. W.; Schlegel, H. B.; Scuseria, G. E.; Robb, M. A.; Cheeseman, J. R.; Montgomery, J. A., Jr.; Vreven, T.; Kudin, K. N.; Burant, J. C.; Millam, J. M.; Iyengar, S. S.; Tomasi, J.; Barone, V.; Mennucci, B.; Cossi, M.; Scalmani, G.; Rega, N.; Petersson, G. A.; Nakatsuji, H.; Hada, M.; Ehara, M.; Toyota, K.; Fukuda, R.; Hasegawa, J.; Ishida, M.; Nakajima, T.; Honda, Y.; Kitao, O.; Nakai, H.; Klene, M.; Li, X.; Knox, J. E.; Hratchian, H. P.; Cross, J. B.; Adamo, C.; Jaramillo, J.; Gomperts, R.; Stratmann, R. E.; Yazyev, O.; Austin, A. J.; Cammi, R.; Pomelli, S.; Ochterski, J. W.; Ayala, P. Y.; Morokuma, K.; Voth, G. A.; Salvador, P.; Dannenberg, J. J.; Zakrzewski, V. G.; Dapprich, S.; Daniels, A. D.; Strain, M. C.; Farkas, O.; Malick, D. K.; Rabuck, A. D.; Raghavachari, K.; Foresman, J. B.; Ortiz, J. V.; Cui, Q.; Baboul, A. G.; Clifford, S.; Cioslowski, J.; Stefanov, B. B.; Liu, G.; Liashenko, A.; Piskorz, P.; Komaromi, I.; Martin, R. L.; Fox, D. J.; Keith, T.; Al-Laham, M. A.; Peng, C. Y.; Nanayakkara, A.; Challacombe, M.; Gill, P. M. W.; Johnson,

B.; Chen, W.; Wong, M. W.; Gonzalez, C. Pople, J. A. *Gaussian 03, Revision B.05*; Gaussian Inc.: Pittsburgh, PA 2003.

(10) Thayer, A. M. Fabulous Fluorine. *Chem. Eng. News* **2006**, *84* (23), 15–24, and 27–32.

(11) Lyssenko, K. A.; Antipin, M. Yu.; Antonov, D. Yu. *ChemPhysChem* **2003**, *4*, 817–823.

(12) Lightner, D. A.; Gurst, J. E.; *Organic Conformational Analysis and Stereochemistry from Circular Dichroism Spectroscopy*; Wiley-VCD: New York, 2000; Chapter 4, pp 63–95.

(13) (a) Giorgio, E.; Minichino, C.; Viglione, R. G.; Zanasi, R.; Rosini, C. *J. Org. Chem.* **2003**, *68*, 5186–5192. (b) Giorgio, E.; Viglione, R. G.; Zanasi, R.; Rosini, C. *J. Am. Chem. Soc.* **2004**, *126*, 12968–12976. (c) Polavarapu, P. L. *J. Phys. Chem. A* **2005**, *109*, 7013–7023. (d) Polavarapu, P. L. *Chirality* **2006**, *18*, 343–356.

(14) Ma, B.; Lii, J.; Allinger, N. L. *J. Comput. Chem.* **2000**, *21*, 813–825.

(15) Stephens, P. J.; Devlin, F. J.; Pan, J. J. *Chirality* **2008**, *20*, 643–663.

(16) Freedman, T. B.; Cao, X. L.; Dukor, R. K.; Nafie, L. A. *Chirality* **2003**, *15*, 743–758.

(17) Polavarapu, P. L.; He, J. T. *Anal. Chem.* **2004**, *76*, 61A–67A.

(18) Hansen, A. E.; Bouman, T. D. *Adv. Chem. Phys.* **1980**, *44*, 454–644.

(19) Diedrich, C.; Grimme, S. *J. Phys. Chem. A* **2003**, *107*, 2524–2539.

(20) Polavarapu, P. L. *Mol. Phys.* **1997**, *91*, 551–554.

(21) Kondru, R. K.; Wipf, P.; Beratan, D. N. *J. Am. Chem. Soc.* **1998**, *120*, 2204–2205.

(22) Ernst, L. *Liebigs Ann.* **1995**, 13–17.

(23) Ricci, G.; Ruzziconi, R. *Tetrahedron: Asymmetry* **2005**, *16*, 1817–1827.

(24) (a) Stephens, P. J. *J. Phys. Chem.* **1985**, *89*, 748–751. (b) Stephens, P. J.; Devlin, F. J.; Chabalowski, C. F.; Frisch, M. J. *J. Phys. Chem. A* **1994**, *98*, 11623.

JP9050066